www.czasopisma.pan.pl PAN POLSKA AKADEMIA NAUK www.journals.pan.pl

Arch. Metall. Mater. **64** (2019), 2, 805-812

DOI: 10.24425/amm.2019.127617

S. BUSZTA*, P. MYŚLIWIEC*, R.E. ŚLIWA*#, R. OSTROWSKI*

THE INFLUENCE OF GEOMETRICAL PARAMETERS AND TOOLS MATERIAL ON THE QUALITY OF THE JOINT MADE BY FSW METHOD IN AA2024 THIN SHEETS

The paper presents the results of theoretical analysis and experimental research on the material's influence and tool geometry on the welding speed and mechanical strength of Al 2024 thin sheet metal joints. To make the joints, tungsten carbide and ceramics tools with a smooth and modified surface of the shoulder were used. The choice of the geometrical parameters of the tool was adjusted to the thickness of the joined sheet. During welding, the values of axial and radial force were recorded to determine the stability of the process. The quality of the joint was examined and evaluated on the basis of visual analysis of the surface and cross-sections of the joint area and the parent material, and subjected to mechanical strength tests. The test results indicate that both the geometry of the tool shoulder and the tool material have a decisive influence on the quality of the joint and the welding speed, making it possible to shorten the duration of the entire process.

Keywords: FSW, FSW tools, AA2024, joining of shin sheets

1. Introduction

Friction welding FSW is a complex process of joining metal sheets by bringing them to the state of plasticizing and stirring the material in the joint zone using a suitable tool. This method was developed by the TWI Welding Institute at the University of Cambridge and allows to join materials from ferrous alloys as well as from non-ferrous alloys with particular emphasis on materials resistant to welding by traditional methods [1]. FSW welding is used to join virtually all ferrous and non-ferrous materials and their combinations in a wide range of thicknesses of joined elements. Friction welding allows joining solid-state materials at a temperature of up to 0.9 of the melting point of the combined material [2]. Exceeding this temperature disqualifies the joint due to local partial melting, location of high stresses, discontinuities or cracks in the weld area. Joining elements takes place due to applying a special tool between the joined elements and moving it along the contact line. The heat is generated by friction between the rotating tool and the surface of joined materials. Simultaneously the materials are stirred with a pin (Fig. 1).

Welding process and final effects depend on many factors such as: machine tool, joined material, tool or fastening devices. Parameters which have a direct impact on the quality of joints include, among others, linear speed of welding, tool rotation speed, tool countersink and tool inclination angle. Friction stir welding (FSW) technology is widely used for joining materials such as aluminum and magnesium alloys [4-8] and for joining materials with high melting point such as titanium alloys [9-13].

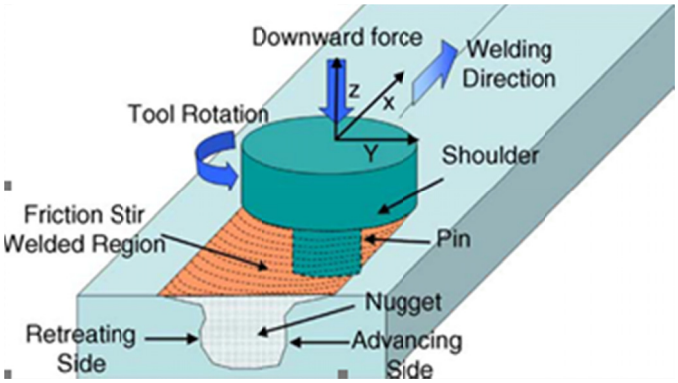

Fig. 1. Schematic illustration of friction-stir welding process [3]

There is little available information about joining thin sheets of metallic materials. Most authors focus on joining metallic material sheets over 2 mm in thickness. So far, there is no adequate information of possible application ceramic materials used for production of FSW tools.

2. Tool's geometry

There are two main parts of tools used in the FSW method and these are the pin and the tool shoulder. The tool shoulder heats the joined material by friction and keeps it in the joint zone, preventing the flow of plasticized material from above the tool shoulder. The shape of the working surface of the shoulder can be

* RZESZÓW UNIVERSITY OF TECHNOLOGY, 8 POWSTAŃCÓW WARSZAWY AV., 35-959 RZESZÓW, POLAND

Corresponding author: rsliwa@prz.edu.pl

flat or concave [15]. In addition, the surface of the shoulder may contain some features that increase friction, in order to increase the degree of stirring of the joined material through the use of grooves with a specific geometry [16]. The pin plays the key role in the deformation and stirring of the material. The pins may be cylindrical or conical in shape, whereas in order to increase the stirring of the joined material, modifications are applied through the use of various types of threads, cuts and grooves [17].

3. Tool's material

The properties of the obtained weld and the degree of wear of the tool are two important issues taken into consideration when selecting the tool material whose properties may affect the quality of the weld by generating and dissipating heat during the welding process. Additionally, the tool material may affect the microstructure of the weld. For joining light materials, such as aluminum, magnesium and copper alloys in the FSW process, steel tools are most often used, less frequently those made of other materials. For joining other materials, tools made of PCBN, tungsten carbide, tungsten alloy with rhenium, less frequently PCD [18-26] are used. In general, the choice of tool materials depends on the hardness of the joined material. The materials used for the tools in the FSW process should have the following properties: high strength at high temperatures, creep resistance, strength and dimensional stability, resistance to thermal fatigue, lack of reactivity with joined material, resistance to cracking, and low coefficient of thermal expansion. The coefficient of thermal expansion of the tool material is particularly important in the process of joining thin sheets with thicknesses below 1 mm due to the small dimensional tolerance of the tool, as the tool making a long weld heats up and deforms to such a degree that no further welding is possible. In such cases, additional equipment is used to remove excess heat from the tool and the joined elements, however this solution increases the cost of the entire process.

Thus, it is purposeful to look for such a tool material which would have a low coefficient of thermal expansion, which could allow for dimensional stability of the tool at high temperatures, and a low thermal conductivity coefficient which could increase the stability and efficiency of the FSW process. Ceramics seem to be a promising material for FSW tools and the results of research in this area are presented in this work.

4. Experimental work

The purpose of the work was to study the impact of advanced tool materials and tool geometry on the parameters of the friction stir welding FSW process as well as on the quality of the obtained joints. The material for testing the effectiveness of the use of tools made of ceramics and tungsten carbide were thin sheets of Al 2024 T3 aluminum alloy with a thickness of 1 mm. Table 1 contains the physical properties of this aluminum alloy.

TABLE 1

Selected properties of Al 2024 T3 alloy [27]

Properties	Al 2024 T3
Density	2,78 g/cc
Hardness, Brinell	120
Hardness, Knoop	150
Hardness, Rockwell A	46,8
Tensile Strength, Ultimate	483 MPa
Tensile Strength, Yield	345 MPa
Elongation at Break	18%
Modulus of Elasticity	73,1 GPa
Poisson's Ratio	0.33
Fatigue Strength	138 MPa
Shear Modulus	28 GPa

The tools used for the welding process were made of special tool CKI 10 tungsten carbide and ceramics. Selected properties of carbide are included in Table 2, while Table 3 contains selected mechanical properties of SYALON ceramics.

TABLE 2

CKI 10 carbide properties [28]

ISO	K30-K40
WC%	90,0
Co%	10
TiC/Ta (Nb)C %	—
Density [g/cm^3]	14,45
Hardness [HV30]	1610
Bending strength [N/mm^2]	3600
Grain size [µm]	0,6
Thermal conductivity [W/(m*K)]	110
Thermal Expansion Coefficient [µm · m^{-1} · K^{-1}]	5.5 µm · m^{-1} · K^{-1}

Tools for the implementation of the process were designed and made of tungsten carbide and special tool ceramics having adjusted geometrical parameters (diameter and height of the pin) to the thickness of welded sheets using the relationships presented in the literature [30-32].

The designed tools were shaped on a multi-axis numerical grinder (Fig. 2) with appropriately selected machining parameters, taking into account the properties of forming grinding wheels, in order to obtain the appropriate dimensional accuracy and surface quality of shaped tools.

After grinding, some of the shaped tools were subjected to modification of the surface of the shoulder by laser beam treatment.

Non-consumable cylindrical tools were made of tungsten carbide and tool ceramics. The geometrical parameters of the tools used for testing are shown in Table 4. Modification of the tool geometry **is based on** making a spiral grooves on the shoulder surface.

Linear butt joints were made using 100×200 mm sheet metal samples. The plates were mounted in a special holder bolted to the dynamometer plate (Fig. 3). The welding process was carried out on a numerical milling machine, the tool was

TABLE 3

Selected mechanical properties of different SYALON ceramics variants [29]

	Syalon 050	**Syalon 101**	**Syalon 110**	**Syalon 201**	**Syalon 501**	**Units**
Composition	α/β-Sialon	β-Sialon	β-Sialon/BN	β-Sialon	β-Sialon/TiN	—
Density	3.23	3.24	2.65	3.24	4.01	g/cc
Porosity	0	0	10	0	0	%
Modulus of Rapture at 20°C	800	945	500	825	825	MPa
Modulus of Rapture at 1000°C	750	700	400	750	—	MPa
Weibull Modulus	12	15	10	10	11	—
Young's Modulus of Elasticity	290	288	139	290	340	GPa
Poisson's Ratio	0.23	0.23	0.19	0.23	0.31	—
Hardness (HRA)	94	92	88	92.7	90.5	—
Hardness (Vickers HV50)	19.81 (2020)	14.71 (1500)	11.77 (1200)	16.18 (1650)	13.24 (1350)	GPa (kg/mm^2)
Fracture Toughness K1C	6.5	7.7	3.5	4.5	5.7	MPa*m½
Thermal Expansion Coefficient (0-1200°C)	3.2×10^{-6}	3.0×10^{-6}	3.0×10^{-6}	3.0×10^{-6}	5.6×10^{-6}	K^{-1}
Thermal Conductivity	20	28	27	21	19	W/(m*K)
Thermal Shock Resistance	600	900	800	600	400	ΔTÍC
Max. Use Temp.	1450	1200	1450	1450	700	°C
Electrical Resistivity	1012	1012	1012	1012	7.2×10^{-4}	Ω * cm

TABLE 4

Geometrical features and material of tools used in FSW process

Tool number	WT1	WT2	WT3	WT4
Tool material	tungsten carbide	tungsten carbide	ceramics	ceramics
Shoulder diameter D [mm]	11	11	11	11
Pin diameter d [mm]	3,5	3,5	3,5	3,5
Pin length [mm]	0,94	0,94	0,94	0,94
Pin profile	cylindrical	cylindrical	cylindrical	cylindrical
Shoulder profile	flat	modified	flat	modified
D/d ratio of the tool	3	3	3	3
View of the tool				

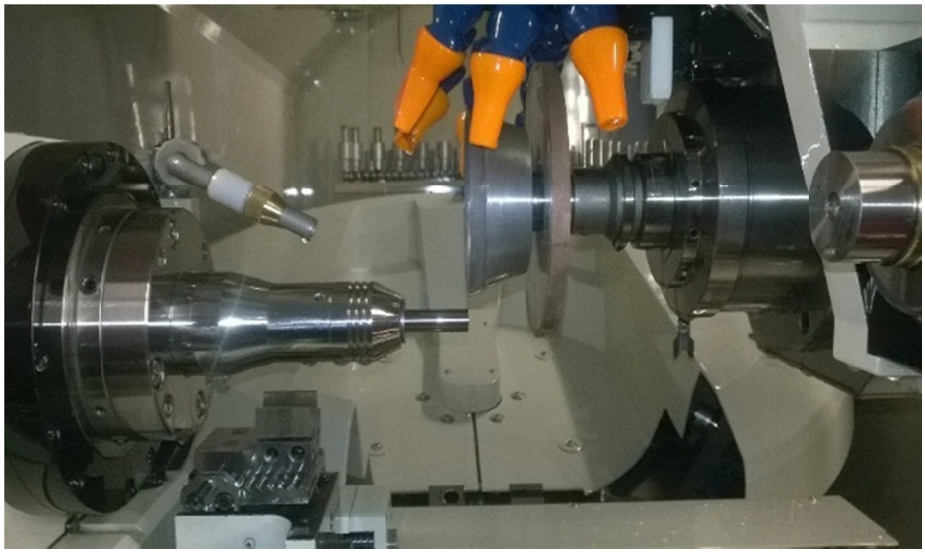

Fig. 2. Shaping tools by grinding on CNC machine to implement the FSW process

not tilted but worked perpendicular to the surface of the joined material.

Welding was performed on a 180 mm long section, under different technological process parameters (welding speed, rotational speed of the tool) in order to obtain the best FSW joint.

The preheating time has been changed (Dwell Time – this is the time of initial plasticizing of the joined material). During welding, the axial force and radial forces as well as the surface temperature of the weld were measured using a thermal imaging camera. Welding conditions and tool parameters used in the tests are included in Table 5.

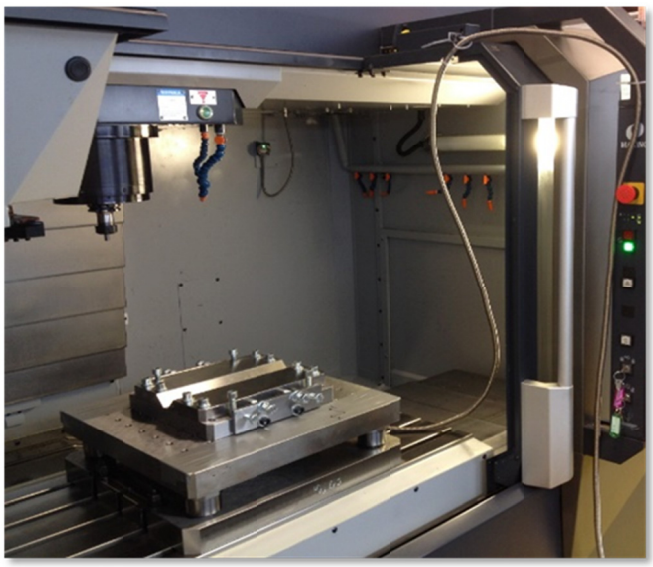

Fig. 3. View of 3 – axis CNC milling machine adopted for realizing FSW process

On the basis of a visual assessment of the surface of the welds (face, ridge) obtained, it can be stated that the best joints are homogeneous and free of defects, both on the face and ridge side of the welded joints. Table 6 shows welds obtained using different shaped tools. On the surface at the welds made with tools with modified surface geometry (spiral groove on the shoulder surface) of the shoulder, there was no occurrence of flash on joined material the welding zone (tools T2 and T4). In welds made with tools with a smooth surface, the flash is clearly visible especially on welds made with the T1 carbide tool. In addition, the surface of welds made with modified tools was matt (no gloss) which may indicate a better flow of welded material during the FSW process.

TABLE 5

Linear FSW technological parameters grouped in relation to welding speed for aluminum alloys sheets

Probe nr	Tool	Rotational speed [rpm]	Welding speed [mm/min]	Dwell time [s]	Plunging [mm/min]
1.	WT2	1750	200	10	6
2.	WT1	2000	200	10	6
3.	WT1	1750	200	10	6
4.	WT4	2000	200	10	6
5.	WT3	1000	200	10	6
6.	WT3	1200	400	4	6
7.	WT3	1200	600	0	6
8.	WT3	1400	900	0	6
9.	WT3	1500	1000	0	6

5. Temperature measurement during FSW process

The temperature was measured using a thermal imaging pyrometer Sirius SI16. The temperature values at the interface surface were dependent on the process parameters and the tool material. Figure 4-6 shows the temperature values on the surface of the weld measured during tests 2, 6 and 9.

TABLE 6

Close-up view of the lateral butt welds made by designed shaped tools

Tool	Face of joint,	Ridge of joint
WT1		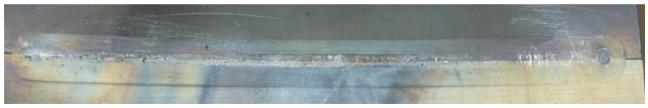
WT2	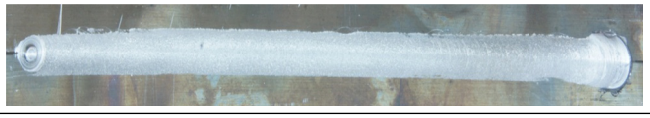	
WT3	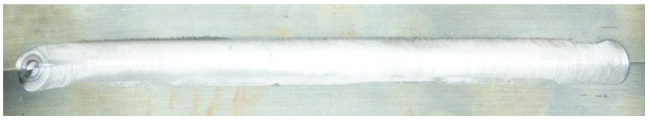	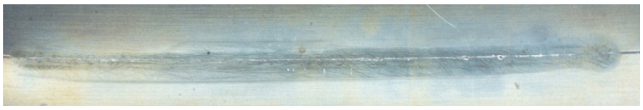
WT4		

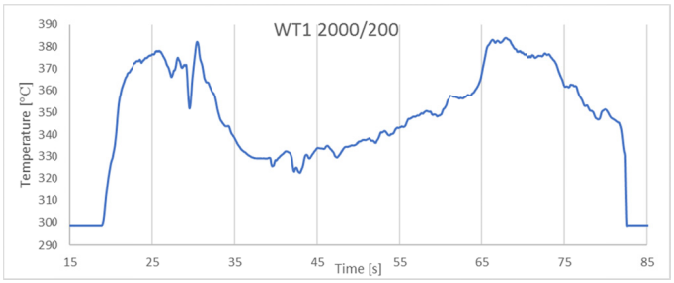

Fig. 4. The temperature value on the surface of the joint AA 2024 T3 sheet of 1mm thickness using carbide tool with smooth shoulder at 2000 rpm and welding speed 200 mm/min (No. 2)

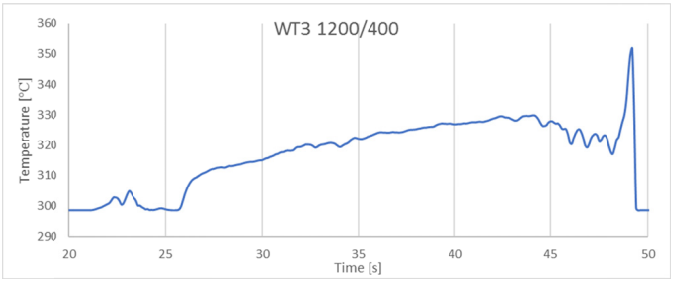

Fig. 5. The temperature value on the surface of the joint of AA 2024 T3 sheet of 1mm thickness using ceramic tool with smooth shoulder at 1200 rpm and welding speed 400 mm/min (No. 6)

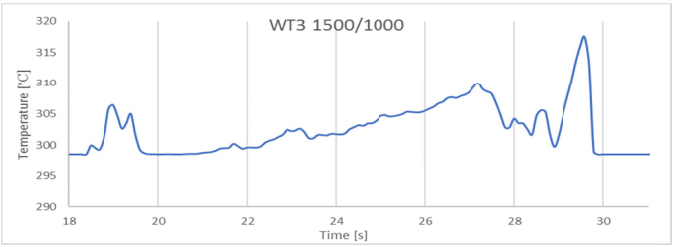

Fig. 6. The temperature value on the surface of the joint of AA 2024 T3 sheet of 1mm thickness using ceramic tool with smooth shoulder at 1500 rpm and welding speed 1000 mm/min (No 9)

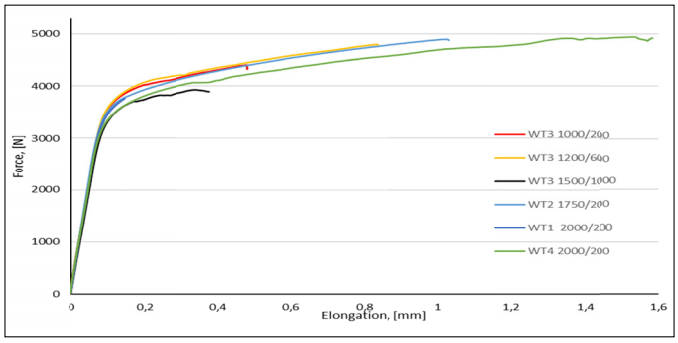

Fig. 7. Tensile test diagram of selected samples of obtained joints of AA 2024 T3 1 mm thickness made by tungsten carbide and ceramic tools with smooth and modified surface of shoulder

TABLE 7

Linear FSW technological parameters, joints and parent material mechanical properties and experimental results for AA 2024 T3 1 mm thickness

Probe nr	Tool	Tool material	Tool geometry	Ultimate tensile strength [MPa]	Joint effective-ness [%]	Joint surface temp.
1.	WT2	tungsten carbide	flat	386	79,91	390
2.	WT1	tungsten carbide	modified	425	87,99	370
3.	WT1	tungsten carbide	modified	423	87,57	370
4.	WT4	ceramics	modified	392	81,15	370
5.	WT3	ceramics	flat	393	81,36	380
6.	WT3	ceramics	flat	341	70,60	366
7.	WT3	ceramics	flat	387	80,12	350
8.	WT3	ceramics	flat	386	79,91	310
9.	WT3	ceramics	flat	309	63,97	300
Parent material				483		

6. Tensile testing of FSW joints

The obtained FSW joints were the basis for making samples to assess the quality of the joints made. The effects of joining the Al 2024 T3 alloy sheets with the tested tools were evaluated on the basis of measurements of axial force and radial forces as well as by measuring the surface temperature of the weld. In addition, the macro and microstructure of the obtained joints were analyzed and the joint strength was measured in a static tensile test on a Zwick / Roell Z100 testing machine at room temperature in accordance with ISO 6892-1: 2009. The ratio of the maximum breaking force of the joint to the parent material was determined, which determines the efficiency of the joint made.

Figure 7 shows the tensile test diagram of selected samples obtained using tools made of cemented carbide and tool ceramics.

The technological parameters of the FSW process, the properties of the welds obtained and the average temperature on the surface of the weld during the process are included in table 7.

7. Micro-hardness tests of FSW joints

The microhardness of the weld was determined by the HV method at 3N load. Measurements carried out on cross-section of the FSW joint. The results of micro-hardness measurements, in case of all welded samples, regardless of the tool, show an increased value in the weld area. In the interface area of the weld the hardness is smallest, however, the decrease in value is small (<5%) in comparison to parent material. Fig. 8 presents diagram of micro-hardness measurement of joints made using carbide tools. The results of microhardness measurements of joints made with ceramic and carbide tools *have not differed* significantly. There was no difference in microhardness of the joints made with tools with a smooth and modified surface of shoulder.

It is visuable small difference in microhardness in the region of FSW joint and parent material area.

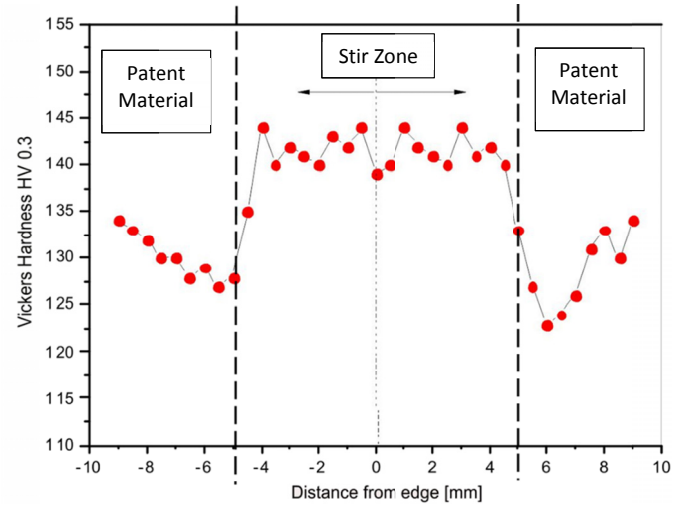

Fig. 8. Diagram of micro-hardness measurement of joint for AA 2024 T3 sheet of 1 mm thickness made by tungsten carbide tool with modified surface of shoulder

8. Microstructure of FSW joints

In order to investigate the microstructure, samples were cut perpendicularly to the welding direction. All received joints were examined. Differences in cross sections of welds made by ceramic tools in relation to welds made by carbide tools were noted. The cross-sectional view of the obtained samples is shown in Figures 9 and 10.

There are no significant differences between the appearance (shape and size) of welds made using different tools. For each sample, the surface of the weld is clean, metallic on the face side and slightly oxidized from the side of the ridge. On the surface of the ridge, in the area of the weld axis, the effects of the welding process are visible, consisting of oxidation and plastic deformation.

In the case of samples made with a carbide tool the shape of the weld in the cross-section is symmetrical with respect to the axis, and the heat affected zone (HAZ) is clearly visible (Fig. 9). In the case of samples made with a ceramic tool the shape of the weld in the cross section shows unsymmetrical (Fig. 10). From the side of the weld in the area directly adjacent to the heat affected zone, there is an area of increased plastic deformation of the alloy, with high density of the flow line. This is most likely related to the conditions of the welding process. The heat affected zone (HAZ) is "fuzzy", poorly visible.

Each of the tested welds, regardless of the tool used, is free from any defects such as pores, cracks or other types of discontinuities that could affect the quality of the joint. The

Fig. 9. Transverse view of a weld made with a carbide tool WT1 joint of AA 2024 T3 sheet of 1 mm thickness using carbide tool with smooth shoulder at 2000 rpm and welding speed 200 mm/min (No. 2)

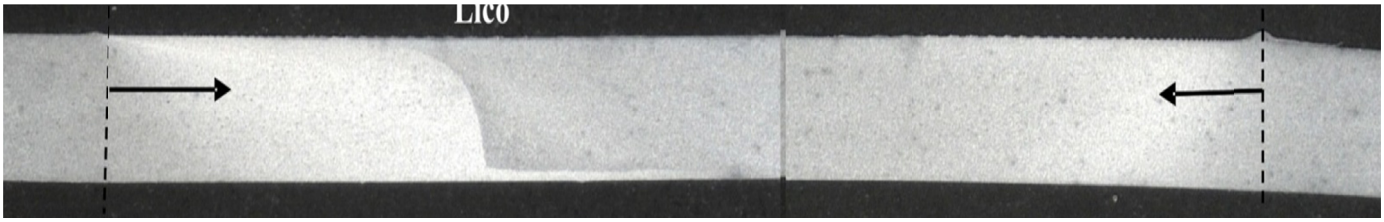

Fig. 10. Transverse view of the weld made with a ceramic tool WT3 joint of AA 2024 T3 sheet of 1 mm thickness using ceramic tool with smooth shoulder at 1000 rpm and welding speed 200 mm/min (No. 5)

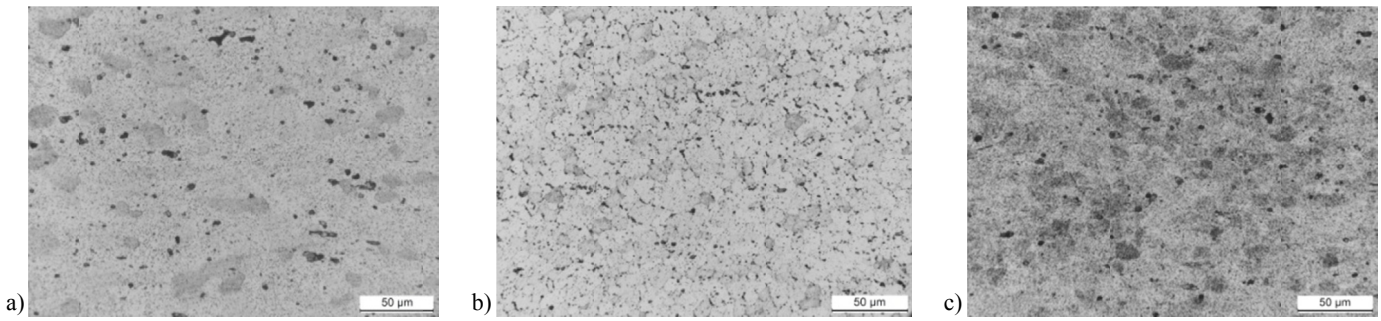

Fig. 11. View of the microstructure a) parent material, b) stir zone of the joint, c) heat affected zone of the joint of AA 2024 T3 sheet of 1 mm thickness using carbide tool with smooth shoulder at 2000 rpm and welding speed 200 mm/min (No. 2)

welding process did not cause significant changes in the alloy microstructure in the area of the weld and adjacent areas. In comparison to the microstructure of the parent material, only a slight increase in grain size in the area of heat affected zone (HAZ) and small fragmentation in the weld area was observed. This phenomenon, however, is a natural effect of processes occurring during welding using FSW technology.

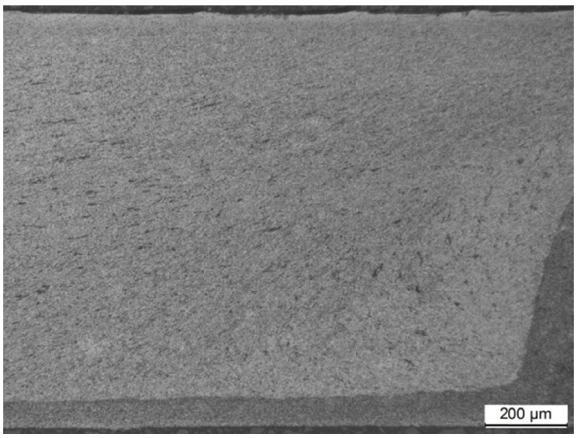

Fig. 12. View of the material flow lines in joint of AA 2024 T3 sheet of 1 mm thickness using ceramic tool with smooth shoulder at 1000 rpm and welding speed 200 mm/min (No. 5)

The microstructure is oriented in terms of the shape of grains and molecules reinforcing the inter-metallic phase (Al-Mg-Cu) according to the plastic flow lines only when the ceramic tool is used in the areas of increased plastic deformation of the alloy.

9. Force measuring during FSW process

The measurements of axial force (Z) and radial forces (X, Y) were made using a specially constructed piezoelectric dynamometer, on which a device for fixing the joined sheets was mounted. Figure 13 shows the results of the measurement of axial and radial forces measured during the welding of of 1 mm thickness using ceramic tool at 1000 rpm and welding speed 200 mm/min (No. 5) due to the highest strength of the joint made by a ceramic tool. The welding was performed using

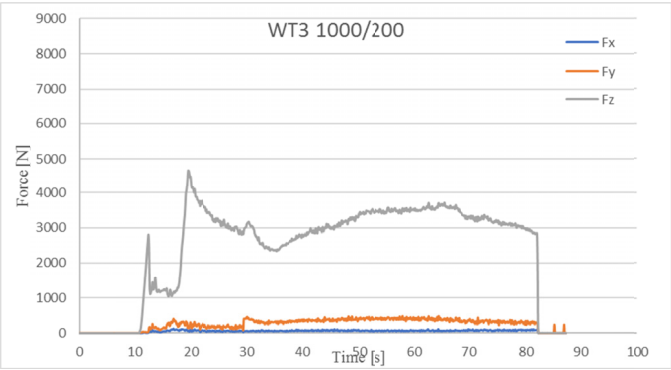

Fig. 13. The welding forces for AA 2024 T3 sheet of 1 mm thickness using ceramic tool at 1000 rpm and welding speed 200 mm/min

ceramic tool with smooth shoulder at 1000 rpm and welding speed 200 mm/min. Figure 14 shows the results of the measurement forces for weld of AA 2024 T3 alloy sheet of 1 mm in thickness (No 9) using ceramic tool with not modified shoulder at the 1500 rpm and welding speed 1000 mm/min. The sample was selected due to the highest welding speed.

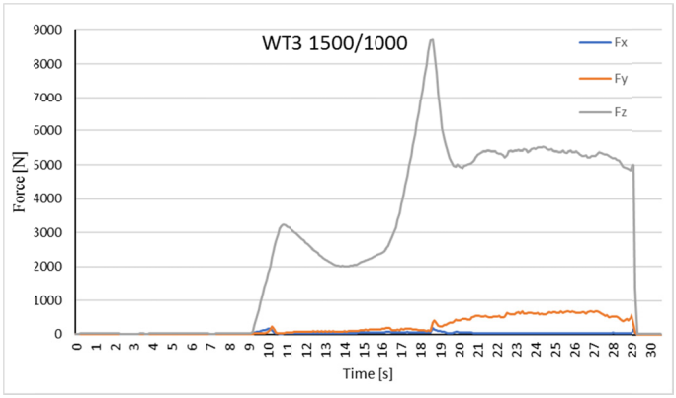

Fig. 14. The welding forces for AA 2024 T3 sheet of 1 mm thickness using ceramic tool at 1500 rpm and welding speed 1000 mm/min

Analyzing the results of force measurements, a significant increase in axial force was observed from approximately 5000 N for the welding speed of 200 mm/min to almost 9000 N for welding speed of 1000 mm/min. Increasing the welding speed brings with it increased welding axial force.

10. Conclusions

Based on the analysis of the research results, the following conclusions were drawn.

1. The shape of the weld in the cross-section is almost symmetrical for carbide tools, for ceramic tools the shape of the weld in the cross-section shows asymmetry on the advancing side, HAZ is “fuzzy”, poorly visible;
2. There is a significant difference in the selection of FSW process parameters for tools made of different materials. The type of tool material and tool geometry have a decisive influence on the effect of joining thin sheets from Al alloys in the FSW process;
3. The applied parameters of the welding process did not affect the quality of the weld in terms of microstructure and hardness distribution. In case of each tested sample, in all separated areas, outside the TMAZ zone, the grain is homogeneous, equi-axial, very fine (a diameter of 3 to 10 µm).
4. FSW welding of thin sheets requires application:
   – the use of a tool with a flat shoulder and thus no tool tilt angle
   – precisely adjusted technological parameters for a given material and sheet thickness
5. The use ceramics for the FSW tool allows for a significant increase in the welding speed and the elimination of dwell

time to zero while maintaining a welding efficiency of 80% compared to the parent material

6. Increasing the welding speed has significantly increased the welding loads in Z direction (tool axis).

REFERENCES

[1] W.M. Thomas, E.D. Nicholas, J.C. Needham, M.G. Murch, P. Templesmith, C.J. Dawes, Friction Stir Butt Welding. International Patent Application PCT/GB92/02203, GB Patent Application 9125978.8. 6 Dec. 1991 and US Patent 5,460,317.

[2] G.G. Roy, R. Nandan, T. DebRoy, Dimensionless correlation to estimate peak temperature during friction stir welding, Science and Technology of Welding and Joining **11**, 5 (2006).

[3] R.S. Mishra, Z.Y. Ma, Materials Science and Engineering R **50**, 1-78 (2005).

[4] Y.S. Sato, H. Kokawa, M. Enomoto, S. Jogan, Microstructural evolution of 6063 aluminum during friction-stir welding, Metall. Mater. Trans. A **30**, 2429-2437 (1999).

[5] Y. Li, L.E. Murr, J.C. McClure, Flow visualization and residual microstructures associated with the friction-stir welding of 2024 aluminum to 6061 aluminum, Mater. Sci. Eng. A **271**, 213-223 (1999).

[6] H.J. Liu, H. Fujii, M. Maeda, K. Nogi, Tensile properties and fracture locations of friction stir welded joints of 2017-T351 aluminum alloy, J. Mater. Proc. Tech. **142**, 692-696 (2003).

[7] S.H.C. Park, Y.S. Sato, H. Kokawa, Effect of micro-texture on fracture location in friction stir weld of Mg alloy AZ61 during tensile test, Scr. Mater. **49**, 161-166 (2003).

[8] D.T. Zhang, M. Suzuki, K. Maruyama, Microstructural evolution of a heat-resistant magnesium alloy due to friction stir welding, Scr. Mater. **52**, 899-903 (2005).

[9] P. Edwards, M. Ramulu, Sci. Technol. Weld. Join. **15**, 468-472 (2010).

[10] P. Edwards, M. Ramulu, Sci. Technol. Weld. Join. **14**, 669-680 (2009).

[11] A. Lauro, Weld. Int. **26**, 8-21 (2012).

[12] G. Buffa, L. Fratini, M. Schneider, M. Merklein, J. Mater, Process. Technol. 213 (2013).

[13] J. Su, J. Wang, R.S. Mishra, R. Xu, J.A. Baumann, Mater. Sci. Eng. A **573**, 67-74 (2013).

[14] A. Fall, Mostafa H. Fesharaki, A.R. Khodabandeh, M. Jahazi, Metals **6**, 275 (2016).

[15] R.S. Mishra, Z.Y. Ma, Friction stir welding and processing. Mater. Sci. Eng. R **50R**, 1-78 (2005).

[16] K.J. Colligan, J.R. Pickens, Friction stir welding of aluminum using a tapered shoulder tool. Friction stir welding and processing, CA, TMS **3**, 161-170 (2005), San Francisco.

[17] R.S. Mishra, M.W. Mahoney, Friction stir welding and processing. Materials Park, OH, 2007, ASM International.

[18] V. RajKumar, et al., Studies on effect of tool design and welding parameters on the friction stir welding of dissimilar aluminium alloys AA 5052-AA 6061. Procedia Engineering **75**, 93-97 (2014).

[19] Charles A. Maltin, et al., The potential adaptation of stationary shoulder friction stir welding technology to steel. Materials & Design **64**, 614-624 (2014).

[20] Joaquin M. Piccini, Hernan G. Svoboda, Effect of pin length on Friction Stir Spot Welding (FSSW) of dissimilar Aluminum-steel joints. Procedia Materials Science **9**, 504-513 (2015).

[21] Nathan, S. Ragu, et al., Effect of welding processes on mechanical and microstructural characteristics of high strength low alloy naval grade steel joints. Defence Technology 11.3 (2015): 308-317.

[22] R. Nandan, T. DebRoy, H.K.D.H. Bhadeshia, Recent advances in friction-stir welding-process, weldment structure and properties. Progress in Materials Science **53**, 6, 980-1023 (2008).

[23] T. Tanaka, et al., Analysis of material flow in the sheet forming of friction-stir welds on alloys of mild steel and aluminum. Journal of Materials Processing Technology **226**, 115-124 (2015).

[24] Nathan, S. Ragu, et al., An investigation on metallurgical characteristics of tungsten based tool materials used in friction stir welding of naval grade high strength low alloy steels. International Journal of Refractory Metals and Hard Materials **56**, 18-26 (2016).

[25] Y. S. Sato, et al., Microstructural evolution of ultrahigh carbon steel during friction stir welding. Scripta materialia **57**, 6 557-560 (2007).

[26] M. Ghosh, K. Kumar, R.S. Mishra, Analysis of microstructural evolution during friction stir welding of ultrahigh-strength steel. Scripta Materialia **63**, 8, 851-854 (2010).

[27] http://asm.matweb.com

[28] http://www.ihle.com/en/hartmetalle-sorten.php

[29] https://www.syalons.com/materials/silicon-nitride-sialon

[30] Y.N. Zhang, X. Cao, S. Larose, P. Wanjara, Review of tools for friction stir welding and processing, Canadian Metallurgical Quarterly **51**, 3 (2012).

[31] A.P. Reynolds, W. Tang, Alloy, tool geometry, and process parameter effects on friction stir weld energies and resultant FSW joint properties, in 'Friction stir welding and processing', 15-23; 2001, Indianapolis, Indiana, TMS.

[32] X.G. Chen, M.D. Silva, P. Gougeon, L. St-Georges, Microstructure and mechanical properties of friction stir welded AA6063-B4C metal matrix composites, Mater. Sci. Eng. A **518**, 174-184 (2009).